

Mechanical properties of Ductile Cast Iron at different carbon equivalent and cast thickness

A.M. Omran¹, G.T. Abdel-Jaber², and A. A. Abdul-Kareem²

1. Mining and petroleum Dept., Faculty of Engineering –Qena, AL-AZhar University, Qena, Egypt
2. Mechanical engineering Dept., Faculty of engineering, South Valley University, Qena, Egypt.

Corresponding Author : mranasser@hotmail.com

ABSTRACT

Recently, Ductile or spheroidal Graphite Iron (SGI) emerged as replacement to other types of cast iron owing to some specific applications. Because, it has a good mechanical properties, better castability, machinability and thermal resistance. This work investigates the mechanical properties of the produced ductile cast iron (SGI) at different CE and different thickness. The results indicated that, Hardness, UTS, and yield strength for all values of the residual Mg increased by increasing CE and at the same CE %, the hardness, UTS, and yield strength decreased by increasing the section thickness from 20 mm to 80 mm. The Maximum hardness UTS, and yield strength values of the produced SGI alloys obtained in this study were 237 HB, 570 Mpa and 319Mpa respectively. Elongation for all values of nodularity decreased by increasing CE, and at the same CE%, elongation increased by increasing the section thickness from 20 mm to 80 mm. Hardness, UTS, and yield strength increased by increasing the pearlite content in the matrix but elongation decreased.

Keywords:

Ductile cast iron, Nodularity, ,Hardness, Tensile strength, Elongation, and Pearlite matrix.

1. INTRODUCTION

Spheroidal graphite iron (SGI), Ductile cast iron and Nodular cast iron are three names to one of cast iron type with graphite in spheroidal shape. Ductile Iron is not a single material, but a family of versatile cast irons exhibiting a wide range of properties which are obtained through microstructure control [1, 2]. The most important and distinguishing microstructural feature of all ductile Irons is the presence of graphite nodules which act as "crack-arresters" and give ductile iron ductility and toughness superior to all other cast iron types, and equal to many cast and forged steels [3, 4]. In order to ensure the spheroidal graphite shape, it is necessary to use some treatment elements. These elements include magnesium, rare earth elements [5,6]. Alloying elements, such as copper, molybdenum, and even aluminum can be used to change the as-cast matrix from ferrite to pearlite. Since, many researches have been done in order to study the factors that effecting SGI production and to study the properties that offered by this kind of cast iron [7-8]. It was found that, the key variables are; chemical composition of the melt, the cooling rate during the solidification, and the types and the amount that the treated alloy used for liquid metal treatment [9]. CGI provides at least 80% higher tensile strength, 40% higher elastic modulus and approximately double the fatigue strength than the conventional grey cast iron [10]. There are a large group of publications describe the opportunity of obtaining various types of the acicular microstructure [11, 12]. Cast iron's properties are changed by adding various alloying elements, or alloyants. Next

to carbon, silicon is the most important alloyant because it forces carbon out of solution. A low percentage of silicon allows carbon to remain in solution forming iron carbide and the production of white cast iron. A high percentage of silicon forces carbon out of solution forming graphite and the production of grey cast iron [13, 14]. Other alloying agents, manganese, chromium, molybdenum, titanium and vanadium counteracts silicon, promotes the retention of carbon, and the formation of those carbides [2, 15]. Nickel and copper increase strength, and machinability, but do not change the amount of graphite formed [16]. The carbon in the form of graphite results in a softer iron, reduces shrinkage, lowers strength, and decreases density [17]. Sulfur, largely a contaminant when present, forms iron sulfide, which prevents the formation of graphite and increases hardness. The problem with sulfur is that it makes molten cast iron viscous, which causes defects [18]. Tensile strengths for conventional Ductile Irons generally range from 60,000 psi (414 MPa) for ferritic grades to over 200,000 psi (1380 MPa) for martensitic grades [19, 20]. Ferritic ductile irons can exhibit elongation of over 25%. Austempered ductile irons exhibit the best combination of strength and elongation [21]. The main objective of this work is to produce SGI alloys in induction furnace and then to be treated by using different Fe–45Si–5.5Mg nodulizers. The characterization of these alloys was accomplished according to their microstructure, image analyzer, and their mechanical properties; hardness, elongation, tensile and yield strengths to provide technical support for the machine parts, roll mill, roll crushing and automobile applications.

2. EXPERIMENTAL

2.1 Materials

Pig iron, steel scarp, carbon, ferro-silicon, copper, and nodulizer materials are used in this work as shown in table 1. The chemical analysis of these materials was determined by using inductively coupled plasma (ICP) model OES, as shown in Table 3.1.

Table 1 Chemical composition of materials used in this study

Element, % Item	C	Si	Ti	Cu	Mg	Mn
Pig iron	4.2	0.2	0.002	0.002	0.001	0.1
Steel scrap	0.2	0.2	0.001	0.0001	0.000 1	0.01
Carbon	90	-	-	-	-	-
Ferro-silicon	0.5	75	-	-	-	0.2
Copper	-	-	-	99.99	-	-
Nodulizer	0.2	45	-	-	5.6	-

2.2. Procedures

Pig iron and steel scrap weighing about 5 kg charged into an alumina crucible attached in high frequency induction furnace and completely melted, then the flux was added to collect the slag. The slag was skimmed and the molten cast iron was held at an elevated temperature at (1400°C) and a melt sample was taken from the melt to CE meter analysis. Thereafter, the chemical composition was adjusted and checked using the carbon equivalent analyzer. Once the main alloy additions were complete, chilled pieces were taken from each melt for chemical analysis before adding the nodulizer. Liquid treatment, using a Fe–Si–Mg nodulizer was performed by directly injecting the nodulizer into the melt within the pouring ladle., the molten metal was poured into the carbon equivalent analyzer crucible at tapping temperature 1400

°C to estimate the CE, C and Si% after adding the nodulizer. After the desired holding times (1, 4, 7, 10 min) the liquid metal poured into the sand mould and chill mould to produce a sample for chemical analysis. The step sand mould allowed for different section thicknesses Figure 1. Once solidified and cooled to room temperature, the specimens taken from the sand mould and cut for metallographic analysis and mechanical testing. The specimens also were cutting according to ASTM to carry out different mechanical.

Surface of the produced SGI specimens is prepared using standard metallographic techniques before the examination, according to ASTM. After preparation, microstructures of the alloy specimens observed under computerized optical microscope (Model: Olympus BX51). The polished specimens taken for optical microscopy. The microstructures, the shape of graphite (nodularity) and percentage of pearlite of the casting were estimated using software program (SG-3000, Yakamao, Japan) and the results were compared with the standard charts. The samples used for hardness test are prepared need two parallel surfaces polished proceeded as similar of that in microscopic examination. The hardness test carried out using Brinell hardness (load 5 Kgf, $\frac{1}{16}$ inch ball diameter and average of three hardness reading are taken. The standard diameter of the tensile specimen must be 3.125mm and 60mm gage lengths



Figure 1 The Sand mould used in this study

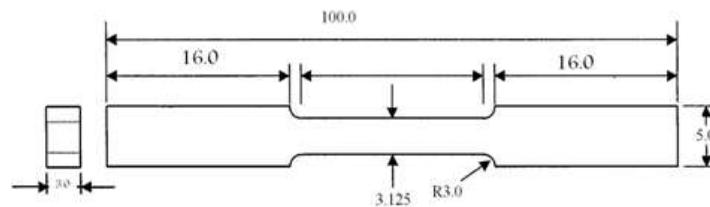


Figure 2 Tensile test specimen according to ASTM

3. RESULTS AND DISCUSSION

3.1 Effect of nodulizer percentages on the nodularity

Nodularity of the produced SGI at different thicknesses of the casting for different nodulizer %, (ranged between 1.7 to 2.9%), and 4.2% carbon equivalent (CE), 4 min. pouring time and 1400 oC melting temperature is shown in Table 3

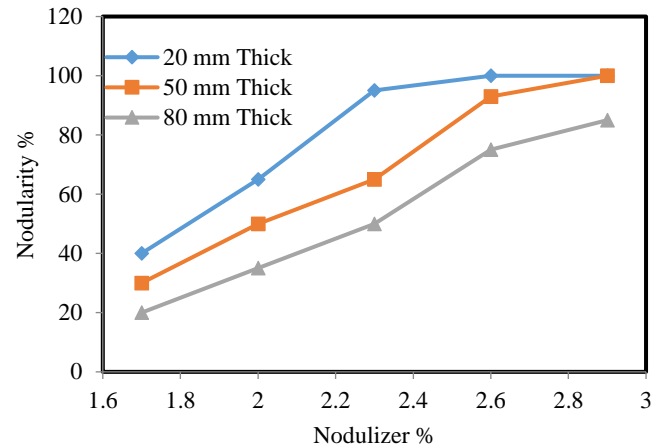


Figure 3 Effect of nodulizer percentages on the nodularity of the produced SGI specimens

The effect of the nodulizer % (Fe-45%Si-5.5%) on the nodularity percentage at different section thicknesses from 20 to 80 mm was investigated from 1.7 to 2.9 as shown in Figure 3. From this Figure it can be seen that the nodularity increases approximately linearly with increasing the nodulizer content in this range, but at the same nodulizer content, the nodularity decreases with increasing the section thickness of the casts. The increasing of nodularity of the produced SGI alloys with increasing nodulizer is a normal result due to increasing of magnesium contents of the melt. But the decreasing in the nodularity percentage with increasing the section thickness is caused by the decreasing in the solidification rate within the section size lead to decreasing of Mg contents in the casts. The nodulizer was found to have the strongest parameter on the nodularity.

A series of micrographs obtained using a light microscopy at 50 mm section thickness for alloys containing different nodulizer contents and different thicknesses are shown in Figure 4. It can be seen from Figure 4.a that the specimen exhibits black nodes or spheres within black vermicular shape. The nodularity measured using image analyzer software and it was 20%, while Figure 4.b, c and d show the micrographs revealing the same matrix structure but different in the amount of the measured nodularity 30, 50 and 65% respectively. Figure 4.e shows full nodules in the matrix contain some of elongated nodules, also, the measured nodularity was 95%. Figure 4.f shows a completely spheroidal shape and the measured nodularity was 100%. It can be conclude that the 100% nodularity obtained by adding the nodulizer more than 2.6 % at section thickness less than 20 mm and the amount of nodulizer more than 2.9% at section thickness less than 80 mm.

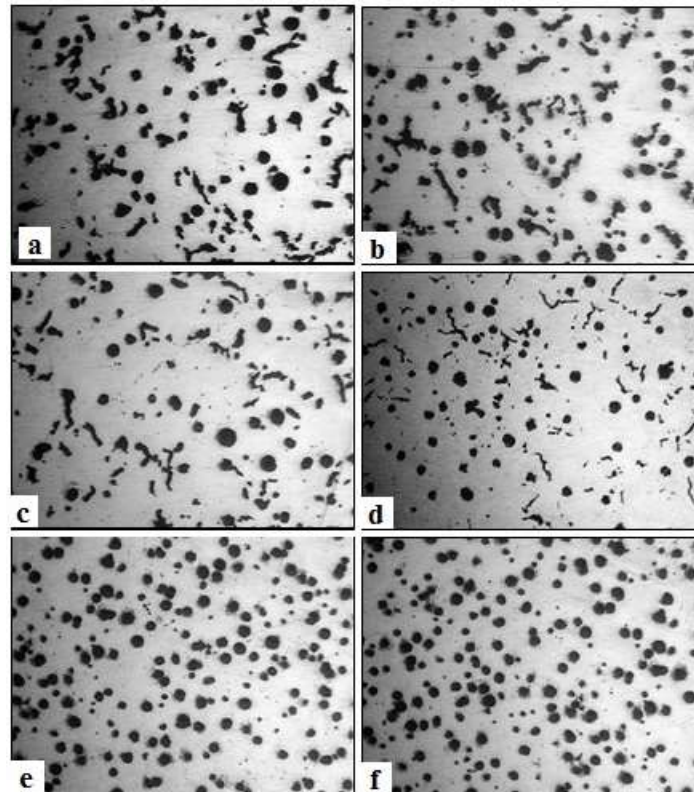


Figure 4 Micrographs of the produced ductile cast iron with different nodulizers percentages
a) 20% b) 30% c) 50% d) 65% e) 95% f) 100%

3.2 Mechanical Properties of the Produced SGI

3.2.1 Hardness of SGI alloys

Hardness of SGI alloys at different contents of residual Mg% (ranged between 0.0155 and 0.031 %) with constant CE (4.2%), Cu (0.1%), Mn (0.1%), pouring time (4 min.) and different cast thicknesses. The effect of the residual Mg % at CE 4.2 % on the hardness of the specimens with section thicknesses of 20, 50 and 80 mm is shown in Figure 5. From Figure 5, it can be seen that the hardness increased as the residual Mg increasing, because the increasing of Mg % in the casts increase the nodularity which is a function of hardness [22]. But at the same Mg contents, the hardness decreases by increasing section thickness due to increasing of solidification time which leads to increasing the losses due to oxidation of Mg. However, after completing the solidification, no much more Mg can be moved out. It is more likely that the better mechanical properties come from the fact that the structure is finer at higher cooling rate of thin section than thick one in thicknesses. Increasing the residual Mg % from 0.0155 to 0.031 % resulted in increasing the hardness from approximately 167 to 258 HB for the 20 mm thick section, from approximately 150 to 231 HB in the 40 mm thick section and from approximately 142 to 206 HB in the 80 mm thick section.

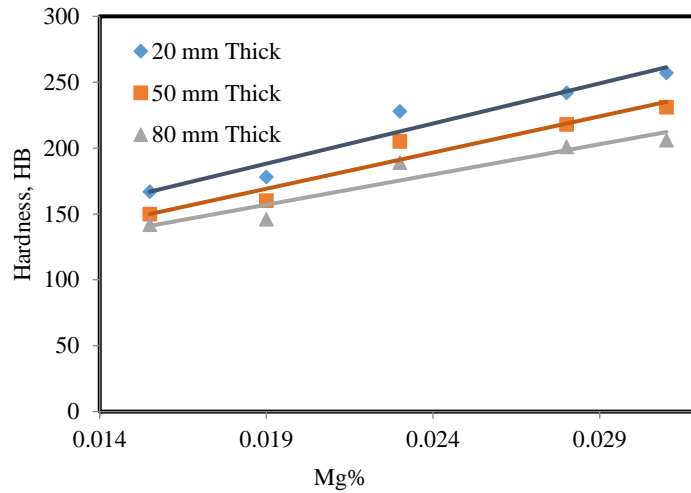


Figure 5 Effect of residual Mg on the hardness of the produced SGI specimens at different cast thicknesses at constant CE (4.2 %)

Figure 6 shows the effect of residual Mg on the hardness of the produced SGI specimens at different CE and at thickness 50 mm. This Figure shows that the hardness increases by increasing the carbon equivalent CE. This increasing, due to the carbon and Si contents that leads to increasing the hardness property. This was confirmed to that published in literature [23]. Increasing the CE also increases the nodularity owing good mechanical properties specially on the hardness.

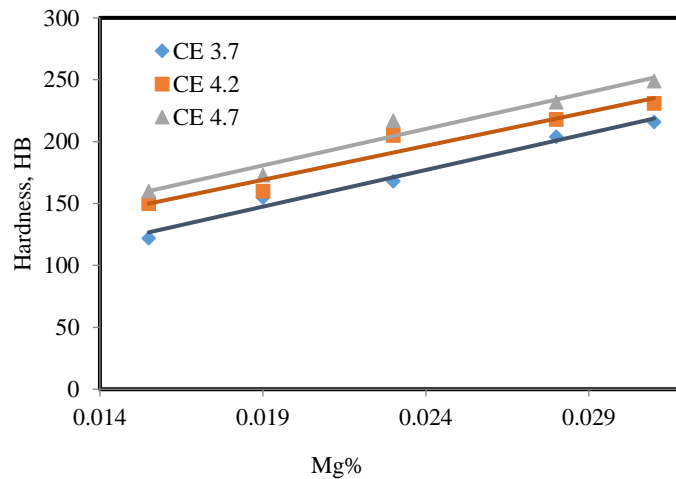


Figure 6 Effect of residual Mg on the hardness of the produced SGI specimens at different CE at section thickness 50 mm.

3.2.2 Ultimate tensile strength of SGI alloys

Ultimate tensile strength (UTS) of SGI alloys at different contents of residual Mg% (ranged between 0.0155 and 0.031 %) with constant CE (4.2%), Cu (0.1%), Mn (0.1%), pouring time (4 min.) and different cast thicknesses. The effect of the residual Mg % at constant CE (4,2%) on the ultimate tensile strength for the specimens with section thicknesses of 20, 50 and 80 mm

is shown in Figure 7. This Figure indicates that the UTS increases as residual Mg content increase for all section sizes, due to increasing the nodularity. For the same Mg content, the UTS decreased by increasing section size. This decrease is due to decreasing the cooling rate, lead to some losses in Mg contents this is in turn decreasing the nodularity. The increasing of residual Mg % from 0.0155 and 0.031 % lead to an increase of the UTS from approximately 357 to 536 MPa for the 20 mm thick section, from approximately 321 to 501 MPa in the 50 mm thick section and from approximately 303 to 440 MPa in the 80 mm thick section.

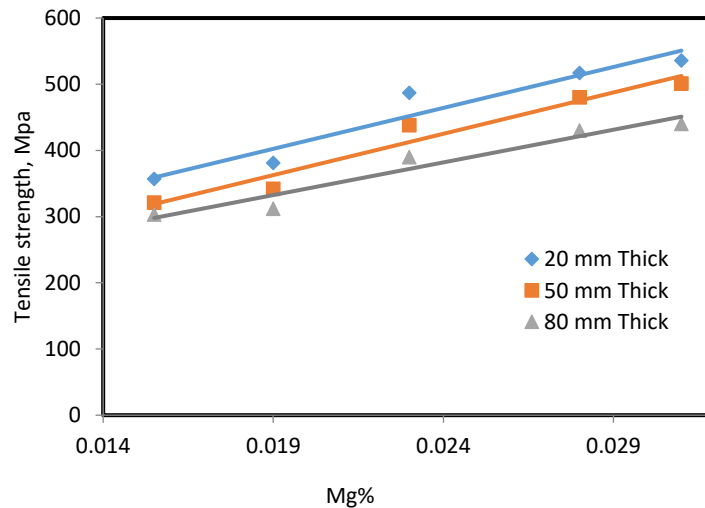


Figure 7 Effect of residual Mg on the ultimate tensile strength of the produced SGI specimens at different cast thicknesses at constant CE (4.2 %).

Figure 8 shows the effect of residual Mg on the UTS of the produced SGI specimens at different CE and at section thickness 50 mm. This Figure shows that the UTS increased by increasing the CE. Also, the UTS increased by increasing the residual Mg in all used CE %.

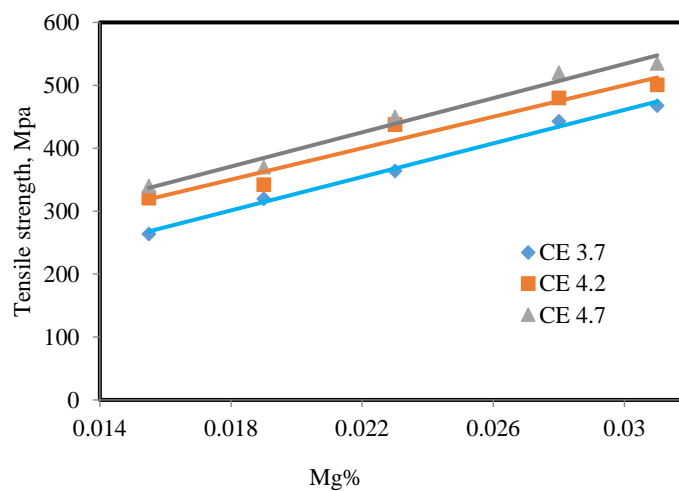


Figure 8 Effect of residual Mg on the ultimate tensile strength of the produced SGI specimens at different CE and at section thickness 50 mm.

3.2.3 Elongation of SGI alloys at different CE

The effect of the residual Mg % at different CE 4.2 on the elongation for the SGI specimens with different casts thicknesses of 20, 50 and 80 mm is shown in Figures 9.

These Figures shows that the elongation decreased by increasing residual Mg content for all section sizes, due to an increase in the nodularity. For the same Mg content, the elongation increased with increasing section size. This increasing is due to increasing of solidification time led to decreasing the cooling rate and in turn increasing of Mg losses. %. Increasing the residual Mg % from 0.0162 to 0.0306 % resulted in an decreased of elongation from approximately 10.0 to 3.0 % for the 20 mm thick section, from approximately 11.0 to 5.0 % for the 50 mm thick section and from approximately 12 to 7.0 % for the 80 mm thick section.

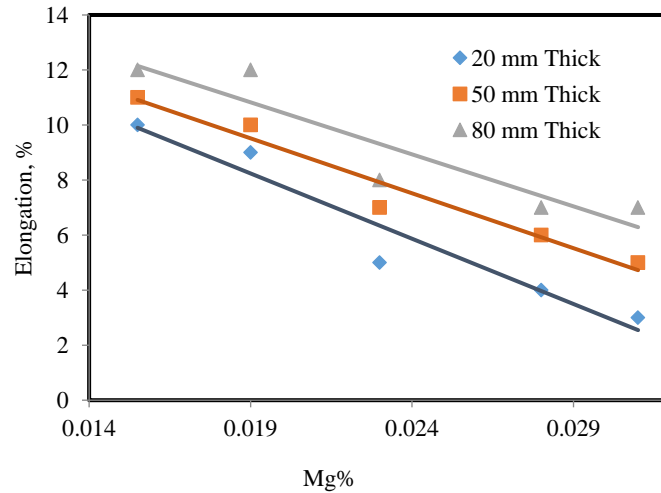


Figure 9 Effect of residual Mg on the elongation of the produced SGI specimens at different thickness for CE 4.2 %

Figure 10 shows the effect of residual Mg on the elongation of the produced SGI specimens at different CE and at section thickness 50 mm. This Figure shows that the elongation decreased by increasing the CE. In addition, the elongation decreased by increasing the residual Mg in all used CE %. Increasing the residual Mg % from 0.0162 to 0.0306 % resulted in an decreased of elongation from approximately 15.0 to 7.0 % for 3.7 % CE, from approximately 11.0 to 5.0 % for 4.2 % CE and from approximately 11.5 to 4.0 % for 4.7 % CE.

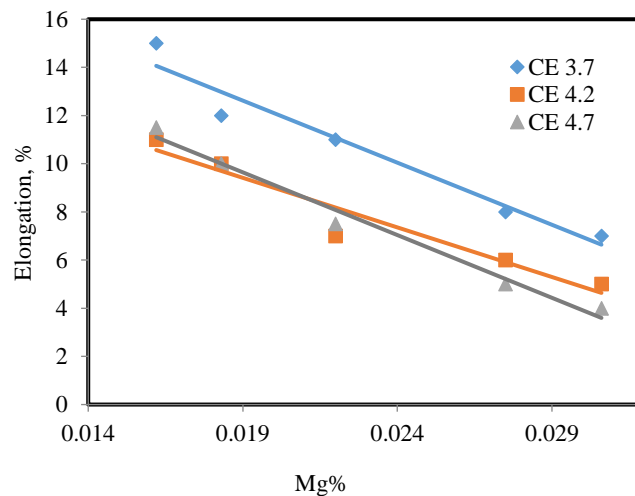


Figure 10 Effect of residual Mg on the elongation % of the produced SGI specimens at different CE for thickness 50 mm

3.2.4 Effect of pearlite contents on Mechanical properties

Figure 11 indicates that the UTS, YTS and Brinell hardness increase as pearlite contents increased, but the elongation decreased as the pearlite contents increased. Because mechanical properties are persistent primarily by the matrix components and their hardness. For the different types of ductile Iron, the matrix consists of ferrite and pearlite. Ferrite is the softest iron phase in ductile Iron. It has high ductility, toughness and good machinability, but low hardness and strength. Pearlite is an entangled mixture of hard lamellar cementite in a ferrite matrix. According to the volume fraction of ferrite and pearlite provides a combination of higher strength and hardness and lower ductility. Therefore, the mechanical properties of ferritic/pearlitic ductile irons are therefore, determined by the ratio of volume fraction of ferrite to pearlite in the matrix. This ratio is controlled in the as-cast form by controlling pearlite stabilizing alloying element such as Cu, Mn and tin which increased the pearlite phase and the cooling rate of the casting [15]

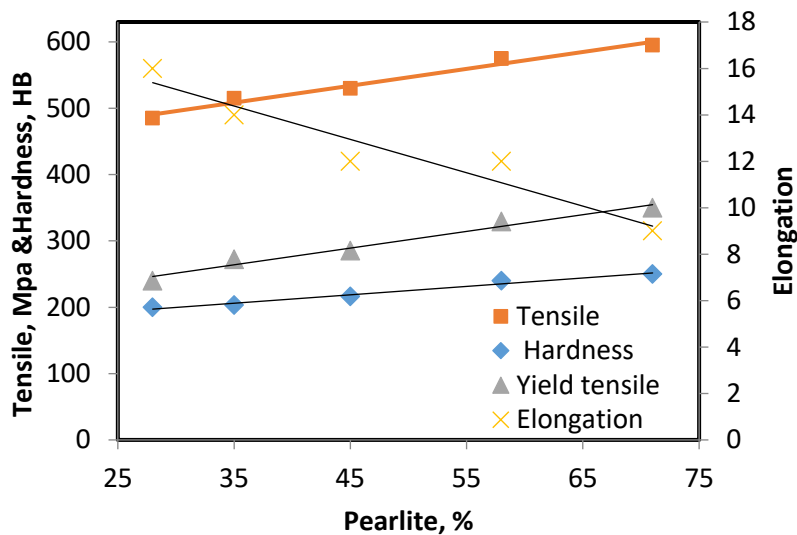


Figure 11 Effect of pearlite contents on the UTS, YTS, Hardness and Elongation of the produced SGI specimens .

4. CONCLUSION

From the results and discussion of the present work, the following items can concluded:

1. Hardness, UTS, and yield strength for all values of CE increased by increasing the residual Mg due to increasing the nodularity, and at the same Mg contents, the hardness, UTS, and yield strength decreased by increasing the section thickness from 20 mm to 80 mm. This decrease is due to decreasing the solidification time.
2. Elongation for all values of CE decreased by increasing the residual Mg due to increasing the nodularity, and at the same Mg contents, elongation increased by increasing the section thickness from 20 mm to 80 mm. This decrease is due to decreasing the solidification time.

3. Maximum hardness values of SGI alloys were obtained with 4.7% CE in this study. Increasing the residual Mg% from 0.0162 to 0.0306 % resulted in increasing the hardness from approximately 178 to 270 HB for the 20 mm thick section, from approximately 160 to 249 HB in the 50 mm thick section and from approximately 152 to 237 HB in the 80 mm thick section.
4. Maximum UTS of SGI alloys was obtained with 4.7% CE at different contents of residual Mg %. Increasing the residual Mg % from 0.0162 to 0.0306 % resulted in an increase in UTS from 371 to 570 MPa for the 20 mm thick section, from approximately 325 to 500 MPa in the 50 mm thick section and from approximately 310 to 488 MPa in the 80 mm thick section.
5. Once the residual Mg % increase from 0.0162 to 0.0306 % resulted in an decreased of elongation from approximately 15.0 to 7.0 % for 3.7 % CE, from approximately 11.0 to 5.0 % for 4.2 % CE and from approximately 11.5 to 4.0 % for 4.7 % CE.
6. Hardness, UTS, and yield strength increased by increasing the pearlite content in the matrix but elongation decreased.

5. REFERENCES

1. R. W. Heine and P. C. Rosenthal, "Principles of metal casting", McGraw Hill Book Co., (1995)
2. H.T. Angus, *Cast Iron: Physical and engineering properties*. London: Elsevier, 2013.
3. Z. Andrsova and L. Volesky, "The potential of isothermally hardened iron with vermicular graphite", COMAT 2012. 21.-22. 11. 2012. Plzeň, Czech Republic, EU. Retrieved May, 25. 2015 from http://www.comat.cz/files/-_proceedings/11/reports/1060.pdf, 2012.
4. http://konsyst.tanger.cz/files/proceedings/metal_07/Lists/Papers/120.pdf.
5. ASTM, *Standard test method for evaluating the microstructure of graphite in iron casting*", Designation: A247– 16a, Current edition approved April 1, 2016. Published April 2016. DOI:10.1520/A0247-16A.
6. "ASM Metals Handbook", Volume 15, Casting: pp. 1445 - 1484.
7. C. Fragassa, N. Radovic, A. Pavlovic, and G. Minak, " Comparison of mechanical properties in compacted and spheroidal graphite irons ", Vol. 38, No. 1 (2016) 45-56, *Tribology in Industry* www.tribology.fink.rs
8. Sugwon Kim, S.L. Cockcroft , A.M. Omran and Honam Hwang, " Mechanical, wear and heat exposure properties of compacted graphite cast iron at elevated temperatures", *Journal of Alloys and Compounds* 487 (2009) 253–257
9. G. Gumienny, B. Kacprzyk, J. Gawroński, *Effect of Copper on the Crystallization Process, Microstructure and Selected Properties of CGI*, *archives of foundry engineering*, 17 (1) (2017) pp51-56
10. R.A.Gonzaga, *Influence of ferrite and pearlite content on mechanical properties of ductile cast irons*, *Materials Science and Engineering: A Volume 567*, 1 April 2013, Pages 1-8.
11. Ductile iron data for Design Engineers website: <https://www.ductile.org/didata/Section3/3part1.htm>
12. D. M. Stefanescu et al., *Tensile Properties of Thin Wall Ductile Iron*, *Tensile Properties of Thin Wall Ductile Iron*, AFS Transactions 02-178, (2002)
13. Jacques lacaze, aline boudot, vale ´ rie gerval, djar oquab, and Henrique santos, *The Role of Manganese and Copper in the Eutectoid Transformation of Spheroidal Graphite Cast Iron*, *Metallurgical And Materials Transactions A Volume 28A*, (1997),pp 2015
14. P. Ferro, A. Fabrizi, R. Cervo, C. Carollo, *Journal of Materials Processing Technology*, Volume 213, Issue 9, September 2013, Pages 1601-1608.
15. Ductile Iron Society, websit: <http://www.ductile.org/didata/Section2 /2intro.htm#> The Casting Advantage.
16. S.C. Murcia, M.A. Paniagua, E.A. Ossa, *Materials Science and Engineering: A, Volume 566*, 20 March 2013, Pages 8-15.

17. R. K. Dasgupta, D. K. Mondal, A. K. Chakrabarti, A. C. Ganguli, *Journal of Materials Engineering and Performance*, August 2012, Volume 21, Issue 8, pp 1728-1736.
18. M. Ramadan, N. El-Bagoury, N. Fathy, M. A. Waly, A. A. Nofal, *Journal of Materials Science*, June 2011, Volume 46, Issue 11, pp 4013-4019.
19. Marcin Górny, Edward Tyrła *Journal of Materials Engineering and Performance*, Volume 22(1) January 2013—300-305.
20. K. Theuwissen, M. Lafont, L. Laffont, B. Viguier, J. Lacaze, *Transactions of the Indian Institute of Metals*, December 2012, Volume 65, Issue 6, pp 627-631).
21. Oscar Marcelo Suarez, Carl R. Loper Jr. *Metallurgical and Materials Transactions A*, August 2001, Volume 32, Issue 8, pp 2131-2133.
22. Serhan karaman, Cem s. Çetinarslan, “ *Manufacturing process of GGG40 nodular cast iron* “ *International Scientific Conference 19 – 20 november 2010*.
23. G. S. Choy, K. H. Choe, K. W. Lee and A. Ikenaga, *J. Mater. Sci. Technol.*, Vol.23 No.1, (2007)97-100.
24. A.M.Omran , G. T. Abdel-Jaber, and M. M. Ali, *Effect of Cu and Mn on the Mechanical Properties and Microstructure of Ductile Cast Iron*, *Int. Journal of Engineering Research and Applications*, Vol. 4, Issue 6, June 2014, pp.90-96